Image Cover Sheet

CLASSIFICATION	SYSTEM NUMBER
UNCLASSIFIED	498995

TITLE

MODELLING AND MEASUREMENTS OF ATMOSPHERIC TURBULENCE OVER LAND

System Number:

Patron Number:

Requester:

Notes:

DSIS Use only:

Deliver to:

Défense nationale National Defence

UNCLASSIFIED

DEFENCE RESEARCH ESTABLISHMENT
CENTRE DE RECHERCHES POUR LA DÉFENSE
VALCARTIER, QUÉBEC

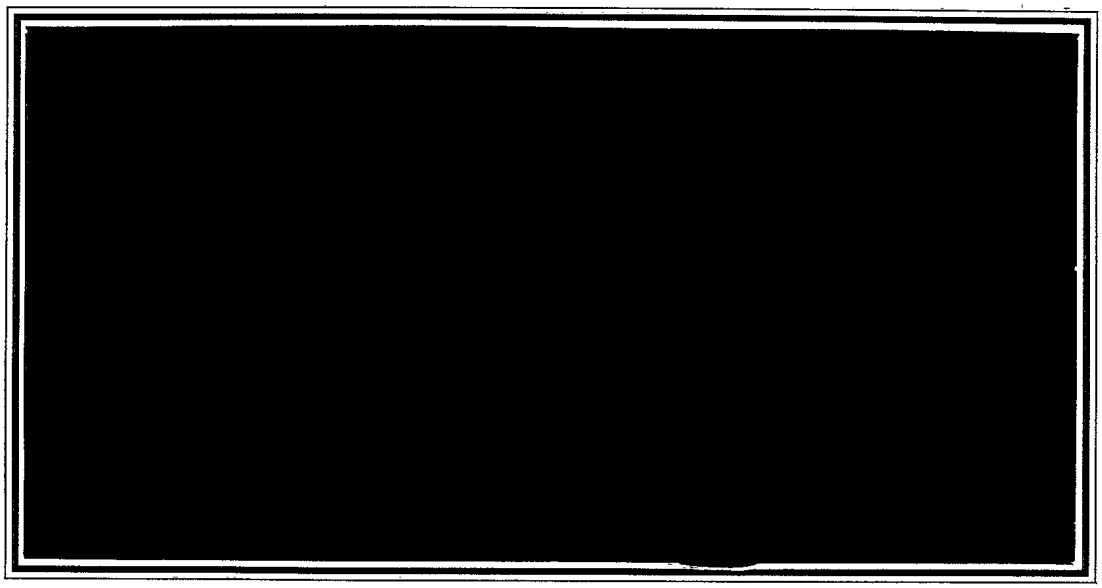

RESEARCH AND DEVELOPMENT BRANCH
DEPARTMENT OF NATIONAL DEFENCE
CANADA
BUREAU - RECHERCHE ET DÉVELOPPEMENT
MINISTÈRE DE LA DÉFENSE NATIONALE

Canada

SANS CLASSIFICATION

UNCLASSIFIED

DEFENCE RESEARCH ESTABLISHMENT VALCARTIER
CENTRE DE RECHERCHES POUR LA DÉFENSE
VALCARTIER, QUÉBEC

DREV - TM - 9604

Unlimited Distribution / Distribution Illimitée

MODELLING AND MEASUREMENTS OF ATMOSPHERIC TURBULENCE OVER LAND

by

D. L. Hutt

July/juillet 1996

Approved by / approuvé par

R. Walker DG

for Chief Scientist / Scientifique en Chef

20/6/96

Date

SANS CLASSIFICATION

ABSTRACT

We present a simple model for the structure constant of atmospheric refractive index fluctuations (C_n^2) and inner scale (ℓ_o) valid in the lowest few hundred meters above land. The inputs to the model are standard meteorological parameters plus solar irradiance and parameters characteristic of the local terrain. Results are compared with measurements of C_n^2 and ℓ_o made with a displaced-beam scintillometer. The results show that the model can predict atmospheric turbulence with good accuracy during daytime.

RÉSUMÉ

Nous présentons un modèle simple de la constante de structure des variations de l'indice de refraction atmosphérique (C_n^2), de taille caractéristique (ℓ_o) et applicable à quelques centaines de mètres au-dessus du sol. Les données d'entrée du modèle sont des paramètres météorologiques standard, auxquels on ajoute le rayonnement solaire et les paramètres caractéristiques du terrain. On compare les résultats obtenus aux mesures de C_n^2 et de ℓ_o effectuées à l'aide d'un scintillomètre. Les résultats montrent que le modèle permet de prévoir les turbulences atmosphériques avec une bonne précision durant le jour.

CONTENTS

EXECUTIVE SUMMARY

The performance of electro-optical systems used for surveillance and target detection can be degraded due to the effects of atmospheric turbulence. The turbulent atmosphere induces slight fluctuations in the direction of light rays propagating over long distances. These fluctuations result in image distortion and blur and may limit the angular resolution of an imaging system. The effect of atmospheric turbulence is often seen as "shimmering" of distant objects seen through binoculars on hot sunny days. Atmospheric turbulence also affects laser beams, inducing intensity scintillation and beam wander, effects that can degrade the performance of target designators and beam riders.

The intensity of atmospheric turbulence is characterized by the refractive index structure parameter C_n^2 which is essentially the standard deviation of differences in the refractive index of air measured simultaneously at two points. This quantity, along with the turbulence inner scale ℓ_o, are sufficient to calculate the optical effects of military significance. This report describes a model that predicts C_n^2 and ℓ_o as a function of ordinary meteorological parameters, solar irradiance and some properties characteristic of the local terrain.

The impact of this work is that atmospheric turbulence can be predicted with a simple model for situations of relevance to the Canadian Land Forces. Such a model can be used in simulations and studies of the effectiveness of EO weapons and surveillance systems. As the angular resolution of EO systems increases, atmospheric turbulence is more frequently the limiting factor in system performance. Furthermore, advances in adaptive optics techniques, currently used in astronomy to dynamically correct images for turbulence effects, will eventually provide technology suitable for land surveillance applications. This report represents a first step in understanding atmospheric turbulence and its effects on EO systems.

1.0 INTRODUCTION

Electro-optical (EO) systems depend on the propagation of light over large distances and are thus susceptible to the influence of optical turbulence. The turbulent atmosphere causes the intensity of a light beam to fluctuate or scintillate, causes beam wander and causes the distortion and random displacement of images. Turbulence can limit the angular resolution of an imaging system to values of hundreds of microradians, many times the diffraction limit of visible imagers, thus resulting in significantly degraded performance (Ref. 1). Predictions of the refractive index structure parameter C_n^2 and the inner scale ℓ_o, the most important parameters which characterize the optical effects of atmospheric turbulence, can be used to predict and optimize the performance of EO systems.

We present a simple model of atmospheric turbulence based on the Monin-Obuhkov similarity theory (Refs. 2 and 3) as interpreted by Thiermann and colleagues in Refs. 4 to 6. The model provides height profiles of C_n^2 and ℓ_o using standard meteorological parameters as inputs. Model results are compared with measurements of C_n^2 and ℓ_o made with a displaced-beam scintillometer installed in a field. The scintillometer provided the path averaged values of C_n^2 and ℓ_o over a 185 m path at a height of 1.8 m. Agreement between the model and measurements are generally quite good under typical daytime conditions. At night, under stable conditions with low wind speed, the model exhibits the instability inherent in the Monin-Obuhkov similarity theory.

This work was carried out at DREV from Jan. 1994 to Dec. 1995 under PSC 32E15 "EO Battlefield Surveillance/Atmospheric Propagation Studies".

2.0 OPTICAL TURBULENCE

When light propagates through turbulent air, it encounters inhomogeneities in the refractive index that transform its phase front. The inhomogeneities are caused by the mixing of air of different temperature by wind and convection. Near the ground, the intensity of temperature fluctuations depends on the type of ground cover, ambient temperature, solar irradiation and wind speed.

Atmospheric turbulence may be characterized by three parameters, the outer and inner scales L_0 and ℓ_o and the refractive index structure parameter C_n^2. The outer scale L_0 represents the minimum scale size over which turbulence energy is injected into the air through

convection or wind shear. Typical values for L_0 are from meters to hundreds of meters. However, in the first few meters above the ground, the surface layer, L_0 is given approximately by L_0=0.4h where h is the height above the ground (Ref. 1). The continuous motion of turbulent air causes the turbulence cells to continuously break up into ever smaller cells until a minimum size ℓ_0 is reached. ℓ_0 marks the turbulence scale size below which viscous dissipation converts the turbulent energy into heat. In the surface layer ℓ_0 is of the order of millimeters. The region between ℓ_0 and L_0 is known as the inertial subrange.

C_n^2 is a measure of the intensity of the refractive index fluctuations. For homogeneous and isotropic turbulence it is defined as (Ref. 1)

$$C_n^2 = \frac{\langle [n(\tilde{r}_1) - n(\tilde{r}_2)]^2 \rangle}{|\tilde{r}_1 - \tilde{r}_2|^{2/3}} , \quad (1)$$

where n is the index of refraction at points $\tilde{r}_1$ and $\tilde{r}_2$. In SI units (used through this paper), C_n^2 has the dimensions of $m^{-2/3}$ and varies from about 10^{-16} to 10^{-12} $m^{-2/3}$ in the atmospheric boundary layer. Equation 1 is valid for distances $|\tilde{r}_1 - \tilde{r}_2|$ much greater than ℓ_0 and much smaller than L_0.

C_n^2 is expressed in terms of the fluctuations in air temperature by (Ref. 1)

$$C_n^2 = \left(\frac{79P}{T^2} \times 10^{-6} \right)^2 C_T^2 , \quad (2)$$

where C_T^2 ($K^2 m^{-2/3}$) is the temperature structure parameter, P is the air pressure in hPa (or millibars) and T is the ambient temperature in degrees K.

The inner scale ℓ_0 (m) is give by (Ref. 6):

$$\ell_0 = 7.4 \nu^{3/4} \varepsilon^{-1/4} , \quad (3)$$

where ν is the kinematic viscosity of air (1.46×10^{-5} m^2/s at STP) and ε (m^2/s^3) is the dissipation rate of turbulent kinetic energy. C_T^2 and ε are provided by the model and Eqs. 2 and 3 are then used to calculate C_n^2 and ℓ_0.

3.0 TURBULENCE MODEL

The solutions for C_T^2 and ε are expressed in terms of the friction velocity u_* (m/s), the turbulent temperature scale T_* (K) and the Monin-Obuhkov length L (m). u_*, T_* and L are scaling parameters defined as (Ref. 6):

$$u_* = uk\left[\ln\left(\frac{z_u}{z_o}\right) - \psi(L)\right]^{-1} \tag{4}$$

$$T_* = -\frac{Q_o}{u_*} \tag{5}$$

$$L = -\frac{u_*^2 T}{kgT_*} \quad . \tag{6}$$

In Eqs. 4 to 6, u (m/s) is the wind velocity measured at height z_u (m) above the ground, z_o (m) is the roughness length of the ground surface, Q_o (Km/s) is the vertical turbulent kinematic heat flux, T is the air temperature measured at height z_u, k (dimensionless) is the Von Karman constant taken to be equal to 0.35 and g is the acceleration of gravity (9.81 m/s^2).

Derivation of the scaling parameters depends upon the form of $\psi(L)$ which is chosen according to whether the conditions are stable (air warmer than the ground) or unstable (air colder than the ground). The $\psi(L)$ are given by (Refs. 5 and 7):

$$\psi(L) = -4.7 z_u/L \qquad z_u/L > 0, \text{ stable} \tag{7}$$

$$\psi(L) = 2\ln\left(\frac{1+y}{2}\right) + \ln\left(\frac{1+y^2}{2}\right) - 2\tan^{-1} y + \frac{\pi}{2} \qquad z_u/L < 0, \text{ unstable} \tag{8}$$

where $y = (1 - 15 z_u/L)^{1/4}$.

During the day Q_o is estimated by (Refs. 5 and 8)

$$Q_o = \frac{\eta}{c_p \rho}\left\{\left(1 - \frac{\alpha}{1+\gamma/s}\right)(1-A)R - \beta\right\} \quad , \tag{9}$$

where η (dimensionless) is an empirical constant equal to 0.9, c_p (J/kg/K) is the specific heat of air, ρ (kg/m^3) is the density of air, α (dimensionless) is a parameter between 0 and 1 that represents the humidity of the ground, γ is the ratio of the specific heat of air at constant pressure to the latent heat of water vapor, s is the temperature derivative of saturation specific humidity. The dimensionless ratio γ/s is a function of temperature only and is tabulated in Ref. 8. A (dimensionless) is the surface albedo, R (W/m^2) is the solar irradiance and β is an empirical constant which we have set equal to 35 W/m^2.

Equation 9 describes how the solar irradiation is partitioned at the ground leaving a component that contributes to the sensible heat flux. The factor (1-A)R is the fraction of solar irradiation absorbed by the ground. Part of this power is dissipated by infrared radiation and ground conduction. This loss is accounted for by the factor η and offset β. The remaining power gives rise to both sensible and latent heat fluxes. The latent heat flux is due to both evaporation at the ground surface and transpiration by vegetation. The fraction of power available for sensible heat flux is determined by the factor $1-\alpha/(1+\gamma/s)$, plotted in Fig. 1. According to Holtslag and Van Ulden (Ref. 8), $\alpha \approx 1$ is an appropriate value for grass covered land as is the case at our location. For dry areas without vegetation (desert), $\alpha \approx 0$. For $\alpha=1$ at a temperature of 25° C, $1-\alpha/(1+\gamma/s)=0.26$ which means that only just over one quarter of the available solar irradiance is transformed into sensible heat flux.

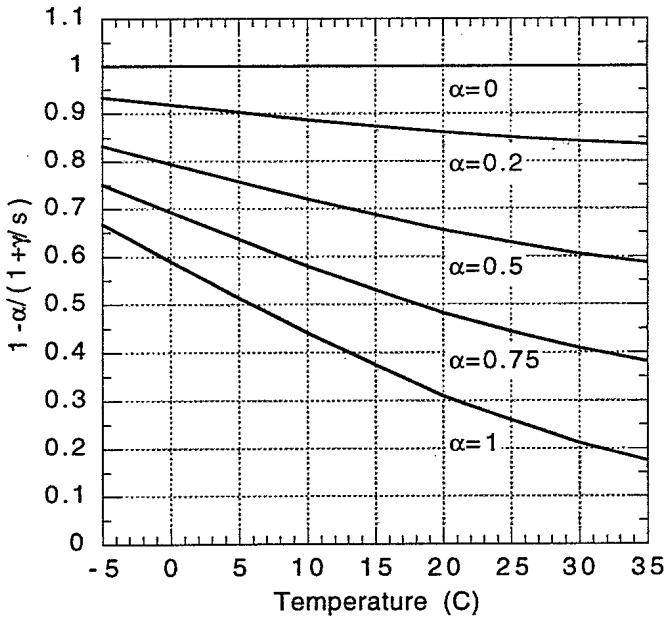

FIGURE 1 Fraction of power available for sensible heat flux as a result of evaporation loss. α is the ground humidity parameter.

The nighttime kinematic heat flux is difficult to estimate because it does not depend on one dominant factor as is the case with solar irradiance for the daytime heat flux. The phenomena on which the nighttime heat flux depends; radiative cooling of the ground, thermal conduction losses and latent cooling or heating due to evaporation or formation of dew, may all have similar importance. Not only is the interaction of these parameters complex but information regarding them would be too specialized for a practical model. To estimate the nighttime heat flux, Thiermann and Kohnle (Ref. 5) developed an expression which depends on the one parameter that is both important and readily available; the wind speed u. The expression is

$$Q_o = \frac{cu^3}{1 + \frac{c}{Q_{omax}} u^3} \tag{10}$$

where $c = \frac{-4}{27} \cdot \frac{k^2 T}{5 g z_u (\ln (z_u/z_o))^2}$.

The structure of Eq. 10 ensures that Q_o does not diverge at high wind speed but increases asymptotically to a saturation value Q_{omax}. This saturation value is given by $Q_{omax} = H_{max}/c_p\rho$ where the sensible heat flux H_{max} is chosen to be between -5 to -100 W/m^2. The most appropriate value of H_{max} depends on local vegetation, ground characteristics, air humidity and cloud cover. For the calculations in this paper we set H_{max} =-12 W/m^2, but as will be shown later, Q_o given by Eq. 10 was in poor agreement with Q_o measured with the scintillometer regardless of the value of H_{max}.

Since the Monin-Obuhkov length L cannot be written as an explicit function of ψ, an iterative procedure must be used to find mutually consistent solutions, u_* and L, to Eqs. 4 to 6. Following Holstag and Van Ulden (Ref. 8), an initial guess for u_* is found by evaluating Eq. 4 with $\psi(L)=0$. L is then estimated by using the initial u_* in Eq. 6. u_* is then reevaluated using L with $\psi(L)$ given by Eqs. 7 or 8, thus beginning a cycle where subsequent values of u_* are compared to the previous one until they are within 0.5% of each other. Typically three to ten iterations are required to determine u_* and L.

The decision as to whether conditions are stable or unstable is based on the value of the daytime heat flux Q_o given by Eq. 9. If the daytime Q_o is positive then conditions are assumed to be unstable and Eq. 8 is used to derive L. If the daytime Q_o is negative then conditions are assumed to be stable, the night time heat flux is calculated using Eq. 10, and Eq. 7 is used to calculate L.

Once the scaling parameters are determined, the vertical profiles of C_T^2 and ε are given by (Ref. 6):

$$C_T^2 = 4\beta \frac{T_*^2}{(kz)^{2/3}} \left[1 + 7\frac{z}{L} + 20\left(\frac{z}{L}\right)^2 \right]^{1/3} \tag{11}$$

$$\varepsilon = \frac{u_*^3}{kz} \left[1 + 4\frac{z}{L} + 16\left(\frac{z}{L}\right)^2 \right]^{1/2} \tag{12}$$

for the stable case (z/L>0) and by

$$C_T^2 = 4\beta \frac{T_*^2}{(kz)^{2/3}} \left[1 - 7\frac{z}{L} + 75\left(\frac{z}{L}\right)^2 \right]^{-1/3} \tag{13}$$

$$\varepsilon = \frac{u_*^3}{kz} \left[\left(1 - 3\frac{z}{L} \right)^{-1} - \frac{z}{L} \right] \tag{14}$$

for the unstable case (z/L<0). the parameters C_n^2 and ℓ_o of interest here are then found substituting C_T^2 and ε into Eqs. 2 and 3.

A multitude of physical quantities are required in the calculations. The specific heat of air c_p is taken to be a constant equal to 1004.6 J/kg/K (Ref. 9). The density of dry air ρ, the ratio γ/s and the kinematic viscosity of air ν are given in following formulae where temperature T is in degrees C:

$$\rho\,(kg/m^3) = 1.286 - 0.00405T \tag{15}$$

$$\gamma/s = 1.4631 - 0.0923T + 0.0027T^2 - 3.18\times10^{-5}T^3 \tag{16}$$

$$\nu\,(m^2/s) = \left(\frac{1.718 + 0.0049T}{\rho}\right)\times10^{-5} \tag{17}$$

Equation 15 is derived from Annex C of Ref. 9, Eq. 16 is a least squares fit to data tabulated in Ref. 8 and Eq. 17 is from Annex C of Ref. 9. The roughness length z_o chosen to represent our location was 0.02 m based on estimated values listed in Ref. 8. The ground humidity parameter α was set at 1. The value of ground albedo A used is 0.2 based on measurements made with a commercial albedometer and is a typical value for grass covered land according to Ref. 8. For the purposes of comparing the model to measured turbulence, we have used the measured solar irradiance R as an input to the model. However R may be easily estimated on the basis of geographic location, time of day and cloud cover. An algorithm to calculate R is given in Annex A.

4.0 TURBULENCE MEASUREMENTS

The experiments were performed at the Defence Research Establishment Valcartier (DREV) in July and August, 1995. The site, known as Parc Lemay, is a level grass covered field with sandy soil. It is about 300 m across, surrounded by spruce trees on the West and North sides and by low buildings on the East. The scintillometer transmitter and receiver were housed in small instrument sheds with a propagation path of 185 m. The path was 1.8 m above the ground and oriented approximately North-South with prevailing winds coming from the West. The layout of the experiment is shown in Fig. 2.

The Scintec SLS-20 scintillometer, used to measure C_n^2 and ℓ_o, is described in detail in Refs. 10 and 11. The SLS-20 uses the independently measured scintillation of two displaced but parallel laser beams to derive the turbulence parameters. The source is a 1 mW laser diode with a wavelength of 670 nm and divergence of approximately 5 mrad. The beam displacement of 2.7 mm is achieved by passing the beam through a birefringent calcite crystal which splits the beam into displaced but parallel components with crossed polarizations. At the receiver the two overlapping beams are resolved by a polarizing beam

splitter, allowing the scintillation of each beam to be measured independently by two 2.5 mm diameter detectors. The transmitted laser beams are modulated at 20 kHz to allow AC coupling of the detector outputs which eliminates the background. The calculations to derive C_n^2 and ℓ_o are carried out in real time by the instruments laptop computer which also derives C_T^2, the kinetic energy dissipation rate, the turbulent fluxes of sensible heat and momentum, and the Monin-Obukhov length using the expressions of Sec. 2. A calibration was carried out for the 185 m path length according to the manufacturer's instructions. The scintillometer receiver is shown in Fig. 3.

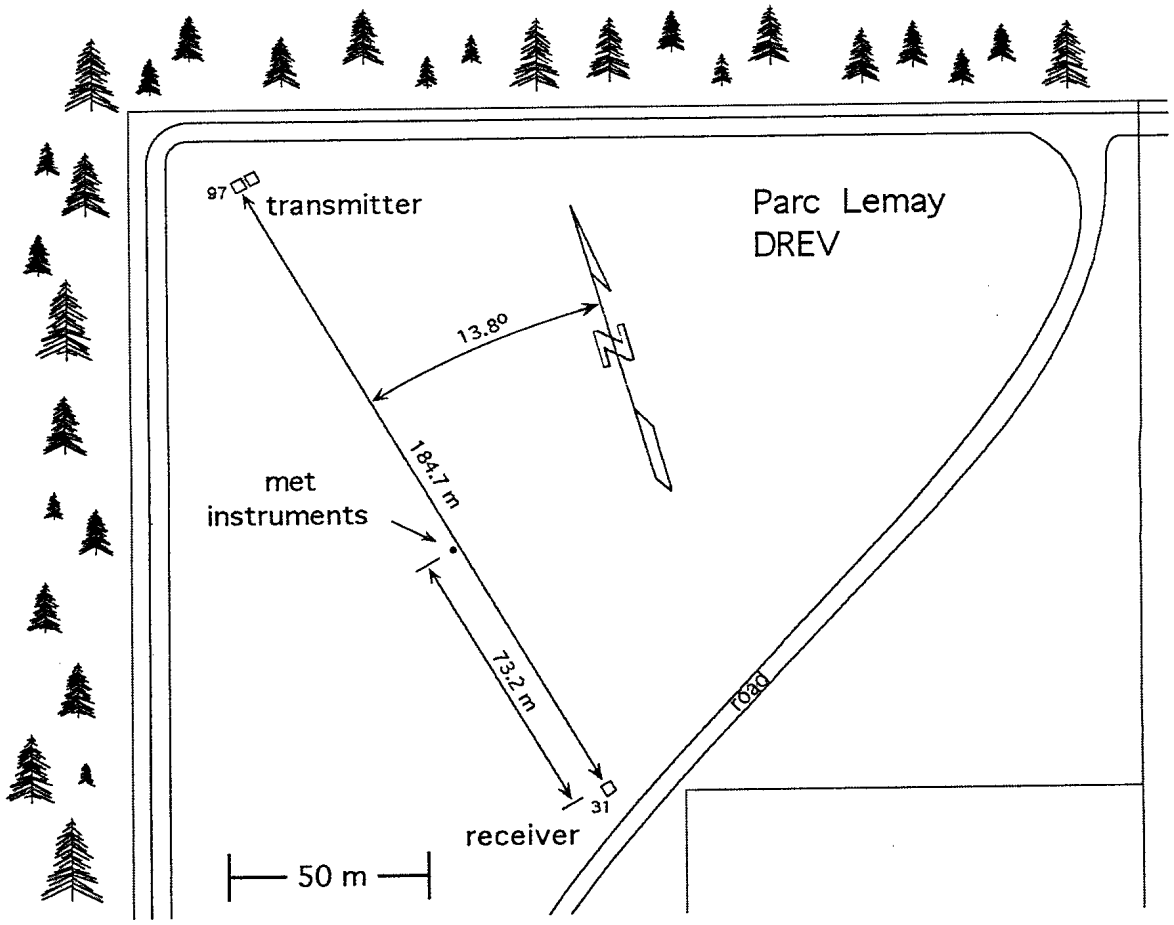

FIGURE 2 Plan of Parc Lemay, DREV, where turbulence measurements were made.

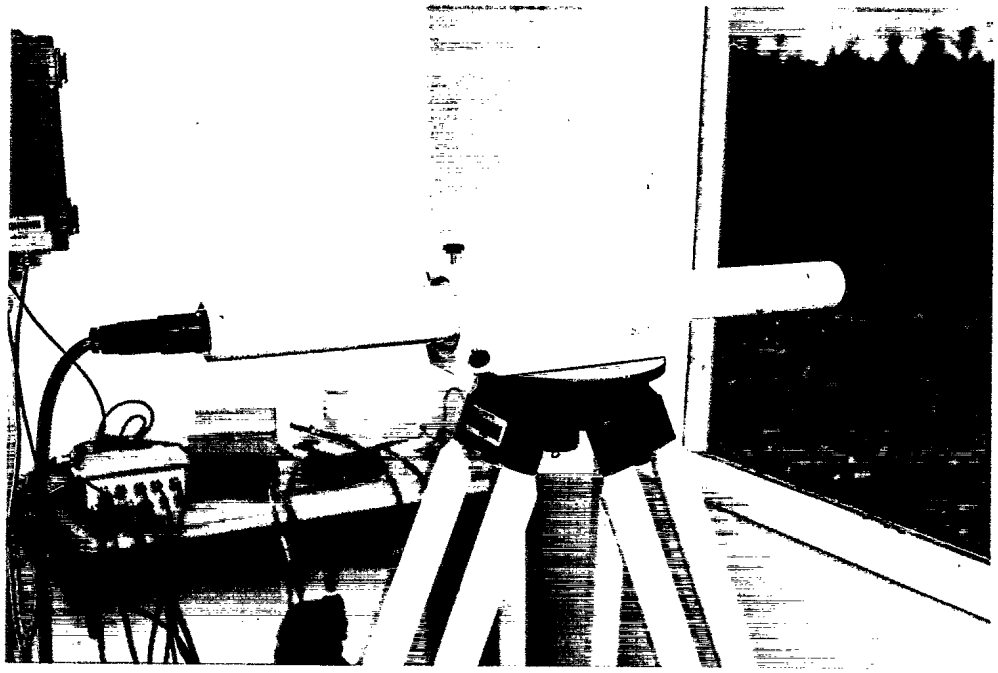

FIGURE 3 Receiver of Scintec SLS-20 scintillometer receiver installed for measurements.

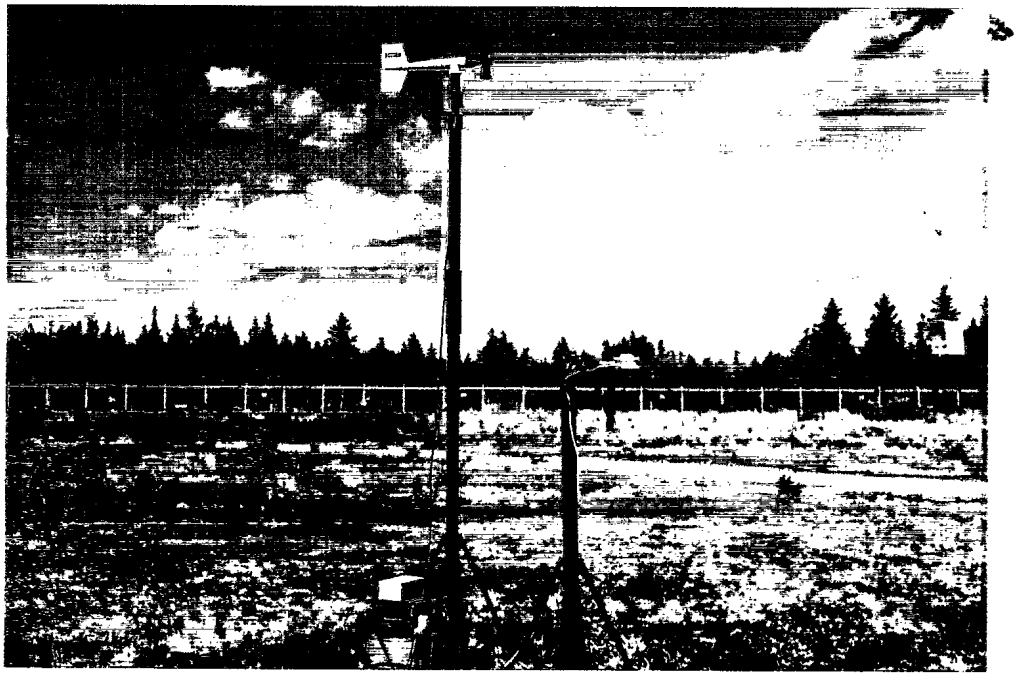

FIGURE 4 The anemometer and the pyrradiometer (for measuring surface albedo) installed near the midpoint of the scintillometer path.

Meteorological conditions were monitored simultaneously near the scintillometer path using standard sensors for wind speed, wind direction, barometric pressure, solar irradiation, air temperature and dew point temperature. The ground albedo was also measured with a pyrradiometer or "albedometer". Some of the instruments and the character of the experiment site are shown in Fig. 4. The wind measurements were made at a height of 3.0 m. The temperature and dew point measurements were made at a height of 1.5 m. The meteorological data was recorded using the SLS-20 analog input channels. The meteorological sensors used are summarized in Table I.

Table I
Meteorological sensors used in experiment

Physical quantity	Instrument name	Manufacturer	Model	Accuracy	Δ time (s)
Wind speed & direction	Wind monitor	Young	05103	±0.25%	not specified
Temperature & dewpoint	Dewpoint & temp. monitor	General Eastern	1200 MPS	± 0.2° C	1.6 °C/s
Atm. pressure	Barometer	Qualimetrics	7105-A	± 1%	not specified
Rain rate	Opt. precip. sens.	STI	ORG-705	± 4%	10
Insolation	Pyranometer	Matrix	R-1950	± 5%	0.001
Ground albedo	Pyrradiometer	Qualimetrics	3040-A	not specified	40

5.0 COMPARISON OF MODEL AND MEASUREMENTS

Figures 6 shows measurements during a four day period from midnight local time Aug. 23 to midnight Aug. 27, 1995. The first day was overcast with subsequent days mostly clear as indicated by the solar irradiance curve (a). Wind speed (b) and relative humidity (c) exhibit diurnal cycles with wind usually less than 3 m/s at night and between 3 and 8 m/s during the day. Humidity was often 100% at night and always less than 75% during the day. No record was kept of the cloud conditions at night.

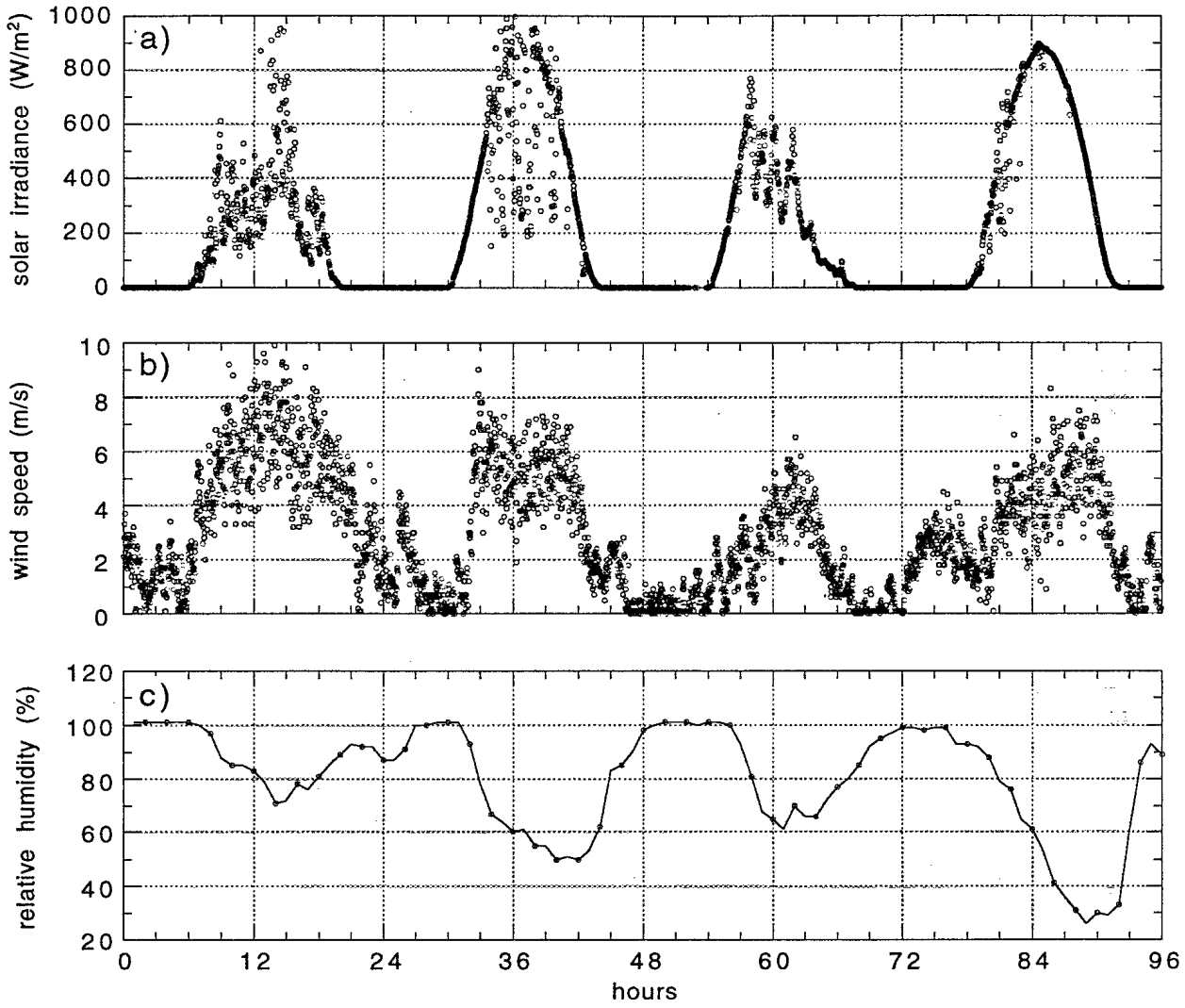

FIGURE 5 Measurements from midnight local time Aug. 23 to midnight Aug. 27, 1995: solar irradiance (a), wind speed at 3 m height (b) and one hour averages of relative humidity (c).

Measurements of C_n^2 and model calculations are shown in Figs. 6 (a) and (b). The calculated C_n^2 follows closely the measured data for daytime periods. At night, the agreement between measured and modelled C_n^2, although reasonably good, is poorer than during the day due primarily to the approximate method of determining the nighttime heat flux based on the wind speed (Eq. 10). Gaps in the nighttime model results occur when the wind speed is less than 0.5 m/s. Below this value, calculations were not performed to avoid inherent instabilities in the Monin-Obukhov similarity theory.

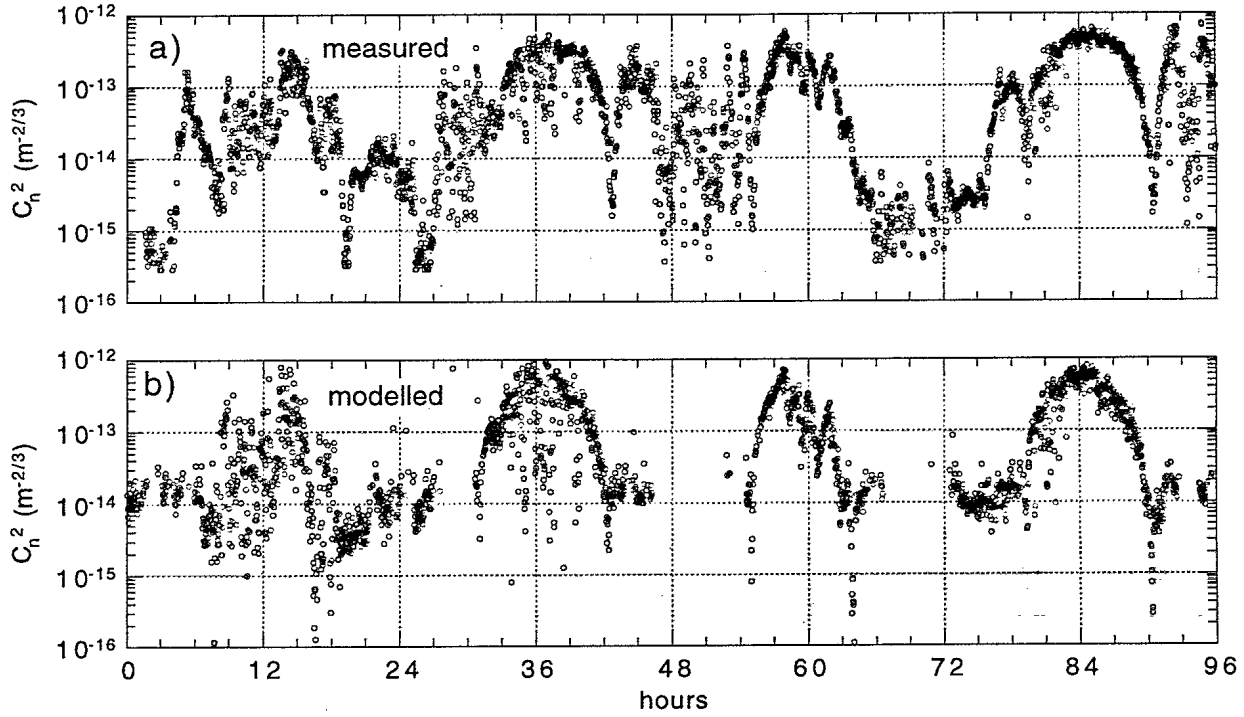

FIGURE 6 C_n^2 measured with SLS-20 scintillometer at 1.8 m height (a), modelled C_n^2 (b).

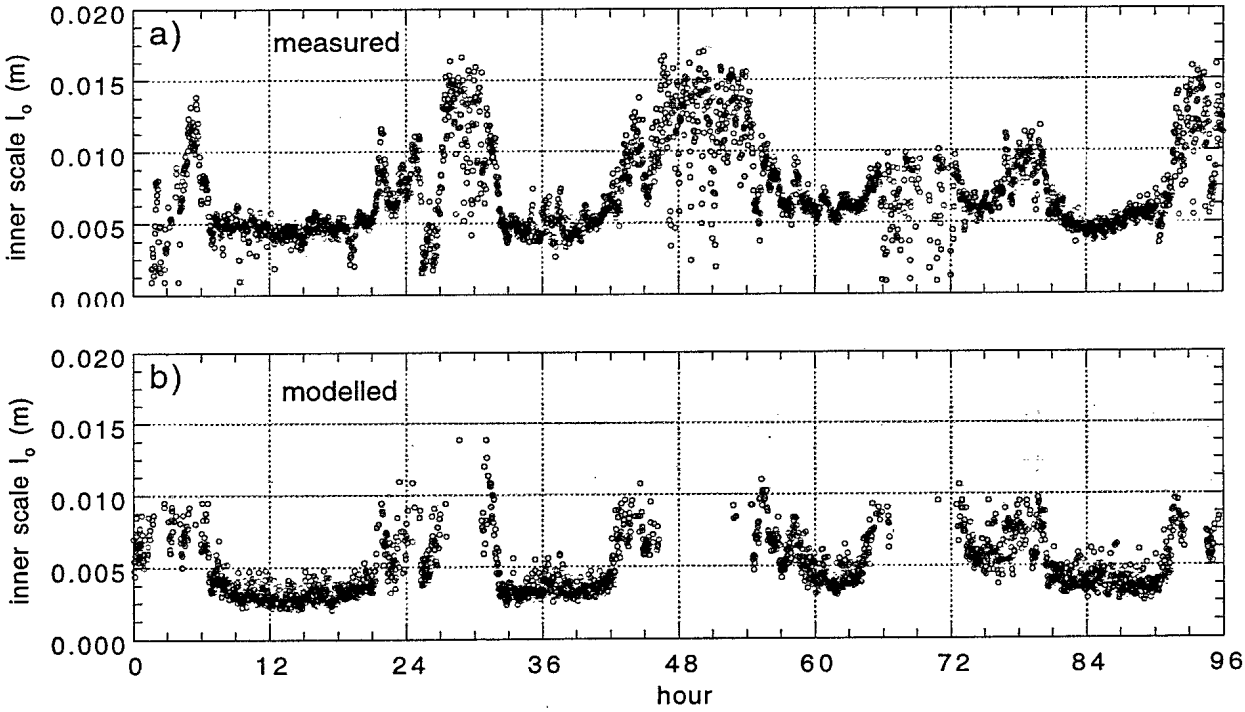

FIGURE 7 Measured and modelled inner scale ℓ_o.

Measurements and model calculations of ℓ_o are shown in Figs. 7 (a) and (b). The relatively large values of ℓ_o during calm night periods and small values during windy day conditions are typical. Agreement between the measurements and model is generally quite good, except at night when the wind speed is less than 0.5 m/s and calculations were not performed. That the model is better able to represent nighttime ℓ_o than C_n^2 is consistent with an analysis by Thiermann and Kohnle (Ref. 5) of the sensitivity of the similarity equations to input errors. They showed that C_T^2, and hence C_n^2, is ten times more sensitive to errors in input Q_o than ℓ_o is.

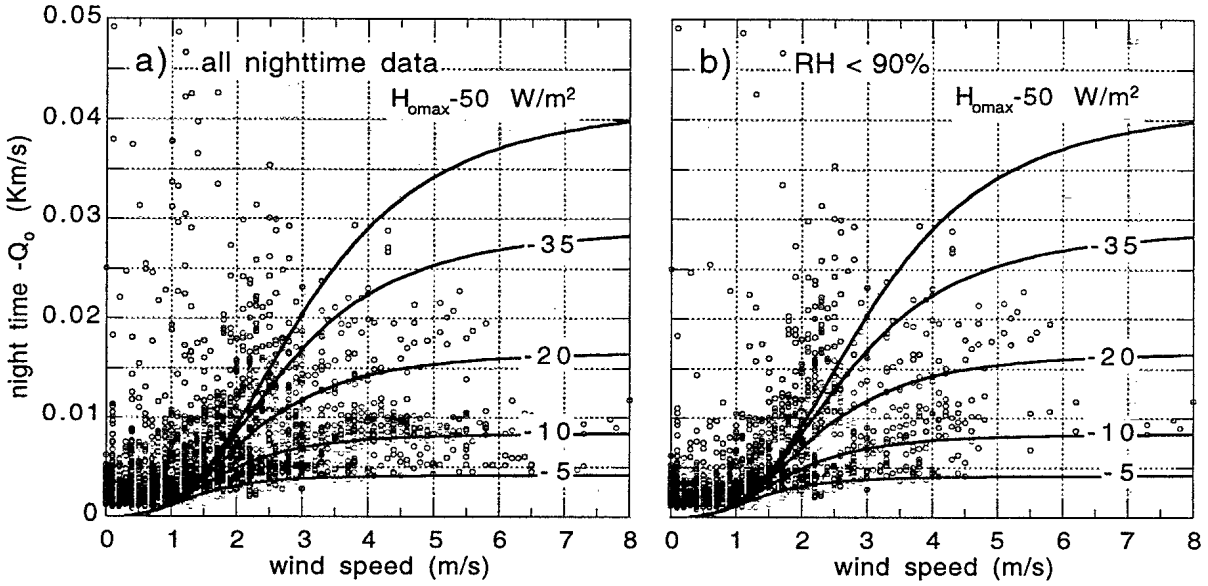

FIGURE 8 Measured nocturnal kinematic heat flux as a function of wind speed. Equation 10 is plotted for several values of saturation heat flux H_{omax}.

The main reason that both the modelled turbulence parameters are in poorer agreement with the measurements at night is because the nighttime heat flux estimated with Eq. 10 is not very accurate. Figure 8 (a) shows the kinematic heat flux measured with the scintillometer as a function of wind speed. The curves are Eq. 10 plotted for various values of saturation heat flux H_{omax}. For our calculations we set H_{omax}=-12 W/m^2 although it is clear from the figure that agreement between the measurements and Eq. 10 is poor regardless of the choice of H_{omax}. The scatter of the data points shows that the nocturnal Q_o has only a vague wind speed dependence under the conditions of our measurements.

The "measured" Q_o shown in Fig. 8 are provided by the Scintec scintillometer software and are derived from the measured C_n^2 and ℓ_o via Eqs. 11 to 14. Therefore, if we choose the same value of Q_o as determined by the scintillometer, the model should produce the same values of C_n^2 and ℓ_o as recorded by the scintillometer.

It is possible that humidity effects play a role in generating heat flux, something which is not taken into account in Eq. 10. The measurements indicate that periods of high C_n^2 at night coincided with 100% relative humidity, for example hours 48 to 54. Dew was usually observed in the mornings, evidence that latent heat was released during the night. Figure 8(b) shows the nocturnal Q_o as a function of wind speed, but with data removed that corresponded with relative humidity greater than 90%. If formation of dew contributed to the measured Q_o then we would expect that the wind speed dependence be more pronounced for data restricted to relatively dry air. However, the Q_o data of Fig. 8 (b) is not significantly better correlated with wind speed than the data of Fig. 8 (a).

Further work is thus required to determine the role (if any) of humidity changes and other possible effects, in generating nocturnal heat flux. An instrument to measure Q_o independently of the scintillometer would be useful in this regard. Estimating the night time heat flux is the weakest part of the model.

6.0 CONCLUSIONS AND FUTURE WORK

We presented results from a simple model for the structure constant of atmospheric refractive index fluctuations (C_n^2) and inner scale (ℓ_o) valid in the lowest few hundred meters above land. The model is based on the Monin-Obuhkov similarity theory (Refs. 2 and 3). The model equations follow Thiermann et. al. (Refs. 4 to 6). The required input parameters are solar irradiance, air temperature, wind speed, barometric pressure and terrain characteristics; albedo, roughness length and ground humidity.

Values of C_n^2 and ℓ_o calculated with the model were in good agreement with measurements made with a displaced-beam scintillometer installed in a field. The scintillometer provided the path averaged values of C_n^2 and ℓ_o over a 185 m path at a height of 1.8 m. The poorest agreement was observed during calm night periods where the model failed to predict the

high levels of intermittent C_n^2 measured by the scintillometer. It is believed that the release of latent heat at night during formation of dew may contribute to the nocturnal heat flux, an effect that was not taken into account. Also, the Monin-Obuhkov similarity theory is inherently unstable for low wind speed and stable night time conditions.

Predictions of C_n^2 and ℓ_o made with this model can be used to predict and optimize the performance of electro-optical systems which are susceptible to the scintillation, beam wander and image distortion caused by optical turbulence over land. Our next effort will be to include humidity fluctuations in the model which will allow C_n^2 to be calculated in the infrared and microwave bands. Also, path-averaged effects on EO systems such as scintillation, point-spread function and image displacement will be included explicitly in the model and compared to measurements of image quality presently being made at the Parc Lemay test site.

7.0 ACKNOWLEDGEMENTS

The author would like to thank M. Luc Gauthier for his technical assistance in setting up the experiments. He also thanks Dr. Volker Thiermann of Scintec GmbH for advice and encouragement.

8.0 REFERENCES

1. Smith, F. G., Ed. 1993. *The infrared & electro-optical systems handbook.* Vol. 2, Section 2.2.6, SPIE Optical Engineering Press, Bellingham.

2. Monin, A. S. and A. M. Obukhov, 1954. "Basic laws of turbulent mixing near the ground." Tr. Akad. Nauk., SSSR Geophiz. Inst., No. 24 (151), 1963-1987.

3. Wyngaard, J. C., 1973. "On surface layer turbulence." *Workshop on micrometeorology*, (Ed. D. A. Haugen). Am. Meteor. Soc. 101-148.

4. Thiermann, V. and A. Kohnle, 1988. "A simple model for the structure constant of temperature fluctuations in the lower atmosphere." J. Phys. 21, S37-S40.

5. Thiermann, V. and A. Kohnle, 1989. "Modelling of optically and IR effective atmospheric turbulence." AGARD CP-454, paper 19.

6. Thiermann, V. and H. Grassl, 1992. "The measurement of turbulent surface layer fluxes by use of bichromatic scintillation." Boundary-Layer Meteor. 58, 367-389.

7. Businger, J. A., J. C. Wyngaard, Y. Izumi and E. F. Bradley, 1973. "Flux-profile relationships in the atmospheric surface layer." J. Atm. Sci. 28, 181-189.

8. Holtslag, A. A. M. and A. P. Van Ulden, 1983. "A simple scheme for daytime estimates of the surface fluxes from routine weather data." J. Clim. Appl. Meteor. 22, 517-529.

9. Stull, R. B., 1988. *An introduction to boundary layer meteorology.* Kluwer Academic Publishers, Boston.

10. Thiermann, V., 1992. "A displaced-beam scintillometer for line-averaged measurements of surface layer turbulence", 10th Symposium on Turbulence and Diffusion, Portland, Or.

11. Hutt, D. L. and F. Trépanier, 1995. "Surface layer turbulence measured with the Scintec SLS-20 scintillometer", Proc. SPIE 2471 Atmospheric Propagation and Remote Sensing IV, Orlando, FL, pp. 461-470.

ANNEX A

CALCULATION OF GROUND LEVEL SOLAR IRRADIANCE

The solar irradiation R at the ground can be estimated for a given time, date and geographical location by calculating the solar elevation angle θ which is the angle of the sun above the local horizon. The downwelling radiation at the surface is then given by:

$$R = ST\sin\theta \qquad \text{for daytime } (\theta \text{ positive}) \qquad \text{(A1)}$$
$$R = 0 \qquad \text{for nighttime } (\theta \text{ negative})$$

where S is the solar constant or the intensity of solar radiation at the top of the atmosphere and T is the sky transmissivity. S will be taken to be 1370 W/m^2 and T is given approximately by (Ref. 9):

$$T = 0.6 + 0.2\sin\theta \ . \qquad \text{(A2)}$$

From Ref. 9, the expression for the local solar elevation angle is

$$\sin\theta = \sin\phi\sin\delta - \cos\phi\cos\delta\ \cos\left(\frac{\pi t_{utc}}{12} - \sigma\right) \qquad \text{(A3)}$$

where ϕ and σ are the latitude (positive north) and longitude (positive west) in radians. δ is the solar declination angle or the angle of the sun above the equator, in radians and t_{utc} is the Coordinated Universal Time in hours. δ is given by:

$$\delta = \phi_r \cos\left(\frac{2\pi\,(d - d_r)}{d_y}\right) \qquad \text{(A4)}$$

where ϕ_r is the latitude of the Tropic of Cancer (23.45^o or 0.409 radians) d is the number of the day of the year (e. g. August 27 is day number 239) and d_r is the day of the summer solstice, 173. d_y is the average number of days in a year, 365.25.

Combining the above expressions and using the geographical location of DREV, ϕ=46°53'5'' (0.818 rad) and σ =71°28'47'' (1.248 rad), yields the solar irradiance curve for August 27 shown in Fig. A1. The data is plotted as a function of local Eastern Daylight Savings time by adding 3.75 hours to t_{utc}.

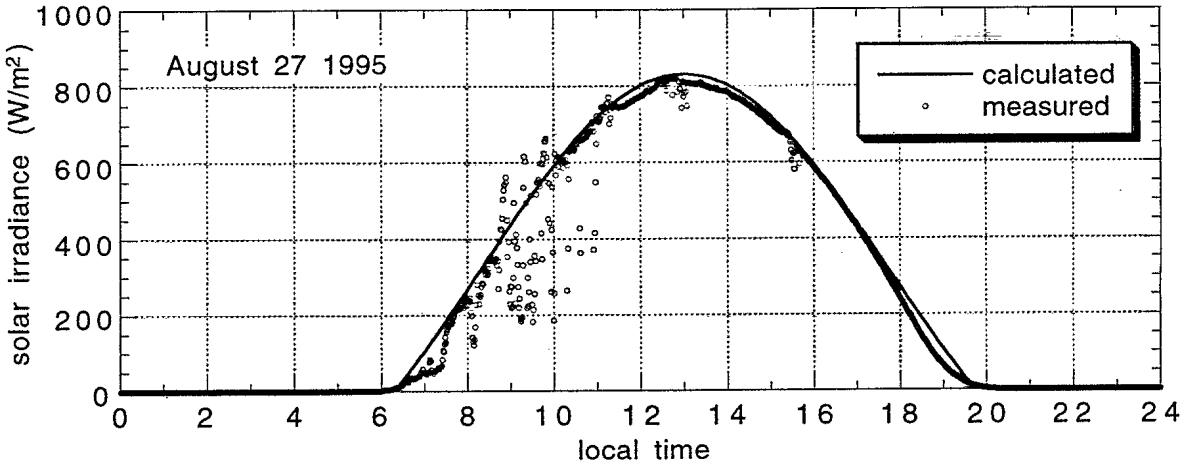

FIGURE A1 Example of calculated and measured solar irradiance at DREV.

August 27, 1995 was a mostly clear day with some thin, high cloud in the morning. It can be seen from the figure that the calculated solar irradiance is in good agreement with the measured values.

The simple model presented here does not take into account the effect of cloud cover. A more elaborate expression for atmospheric transmittance T (Eq. A2) exists but the height and thickness of the clouds must be estimated which is too unreliable for our purposes. More detail on this subject is given in Ref. 9, p. 257. Also, the model does not explicitly take into account the spectral dependence of atmospheric absorption. The semi-empirical expression for T, Eq. A2, applies to the "short wave" solar radiation in the spectral band approximately 0.4 to 2 μm.

INTERNAL DISTRIBUTION

DREV TM-9604

1 - Deputy Director General
1 - Chief Scientist
6 - Document Library
3 - D. Hutt (author)
1 - R. Larose
1 - P. Pace
1 - J. Cruickshank
1 - D. Dion
1 - L. Bissonnette
1 - L. Forand
1 - L. Gauthier
1 - J. Bédard

EXTERNAL DISTRIBUTION

DREV TM-9604

2 - DSIS
1 - CRAD
1 - DREA
1 - DREO
1 - DRES
1 - DCIEM
1 - DLR-2
1 - DSA (L) 5
1 - DLR-4-2-2
1 - DMWOP-2

1 - Prof. Earl Fjarlie
Royal Military College of Canada
Kingston, ON
K7K 5L0

1 - Prof. George Aitken
Dept. of Electrical and Computer Engineering
Walter Light Hall, Queens University
Kingston, ON
K7L 3N6

1 - Mr. Brian Rice
Land, Space & Optoelectronics Division
Defence Science and Technology Organisation
PO Box 1500, Salisbury SA 5108
Australia

1 - Mr. Mike Richards
Defence Research Agency, Funtington
Cheesmans Lane
Hambrook, Near Chichester
West Sussex, PO18 8UE
England

1 - Dr. Jon J. Martin
1 - Dr. Jim Gillespie
US Army Research Laboratory, BED
Attn: AMSRL-BE-A
White Sands Missile Range
New Mexico 88002-5501
USA

1 - Dr. Volker Thiermann
Scintec GmbH
Hölderlinstrasse 31
D-72074 Tübingen
Germany

1 - Mr. Gerard Kunz
TNO Physics and Electronics Laboratory
Oude Waalsdorperweg 63
P. O. Box 96864
2509 JG The hague
The Netherlands

UNCLASSIFIED
SECURITY CLASSIFICATION OF FORM
(Highest classification of Title, Abstract, Keywords)

DOCUMENT CONTROL DATA

1. ORIGINATOR (name and address)

Defence Research Establishment Valcartier
P.O. Box 8800
Courcelette, P.Q.
Canada G0A 1R0

2. SECURITY CLASSIFICATION
(Including special warning terms if applicable)

UNCLASSIFIED

3. TITLE (Its classification should be indicated by the appropriate abbreviation (S,C,R or U)
Modelling and Measurement of Atmospheric Turbulence over Land

4. AUTHORS (Last name, first name, middle initial. If military, show rank, e.g. Doe, Maj. John E.)

D.L. Hutt

5. DATE OF PUBLICATION (month and year)	6a. NO. OF PAGES	6b. NO. OF REFERENCES
	21	11

7. DESCRIPTIVE NOTES (the category of the document, e.g. technical report, technical note or memorandum. Give the inclusive dates when a specific reporting period is covered.)

TM: Technical Memorandum

8. SPONSORING ACTIVITY (name and address)

DREV

9a. PROJECT OR GRANT NO. (Please specify whether project or grant)	9b. CONTRACT NO.
2312E15A	
10a.ORIGINATOR'S DOCUMENT NUMBER	**10b. OTHER DOCUMENT NOS.**
	N/A

11. DOCUMENT AVAILABILITY (any limitations on further dissemination of the document, other than those imposed by security classification)

- [x] Unlimited distribution
- [ ] Contractors in appoved countries (specify)
- [ ] Canadian contractors (with need-to-know)
- [ ] Government (with need-to-know)
- [ ] Defence departments
- [ ] Other (please specify) :

12. DOCUMENT ANNOUNCEMENT (any limitation to the bibliographic announcement of this document. This will normally correspond to the Document Availability (11). However, where further distribution (beyond the audience specified in 11) is possible, a wider announcement audience may be selected.)

UNCLASSIFIED
SECURITY CLASSIFICATION OF FORM

13. ABSTRACT (a brief and factual summary of the document. It may also appear elsewhere in the body of the document itself. It is highly desirable that the abstract of classified documents be unclassified. Each paragraph of the abstract shall begin with an indication of the security classification of the information in the paragraph (unless the document itself is unclassified) represented as (S), (C), (R), or (U). It is not necessary to include here abstracts in both official languages unless the text is bilingual).

We present a simple model for the structure constant of atmospheric refractive index fluctuations (Cn2) and inner scale (lo) valid in the lowest few hundred meters above land. The inputs to the model are standard meteorological parameters plus solar irradiance and parameters characteristic of the local terrain. Results are compared with measurements of Cn2 and lo made with a displaced-beam scintillometer. The results show that the model can predict atmospheric turbulence with good accuracy during daytime.

14. KEYWORDS, DESCRIPTORS or IDENTIFIERS (technically meaningful terms or short phrases that characterize a document and could be helpful in cataloguing the document. They should be selected so that no security classification is required. Identifiers, such as equipment model designation, trade name, military project code name, geographic location may also be included. If possible keywords should be selected from a published thesaurus. e.g. Thesaurus of Engineering and Scientific Terms (TEST) and that thesaurus-identified. If it is not possible to select indexing terms which are Unclassified, the calssification of each sould be indicated as with the title.)

Atmospheric turbulence, scintillation, refractive index structure parameter

Requests for documents
should be sent to:

DIRECTOR SCIENTIFIC INFORMATION SERVICES
Dept. of National Defence
Ottawa, Ontario
K1A 0K2
Tel: (613) 995-2971
Fax: (613) 996-0392

NO. OF COPIES / NOMBRE DE COPIES	COPY NO. / COPIE N°	INFORMATION SCIENTIST'S INITIALS / INITIALES DE L'AGENT D'INFORMATION SCIENTIFIQUE
1	1	JC

AQUISITION ROUTE / FOURNI PAR ▶	DREV
DATE ▶	25 Jul 96
DSIS ACCESSION NO. / NUMÉRO DSIS ▶	

DND 1158 (6-87)

National Defence / Défense nationale

498995

PLEASE RETURN THIS DOCUMENT TO THE FOLLOWING ADDRESS:

DIRECTOR
SCIENTIFIC INFORMATION SERVICES
NATIONAL DEFENCE
HEADQUARTERS
OTTAWA, ONT. - CANADA K1A 0K2

PRIÈRE DE RETOURNER CE DOCUMENT À L'ADRESSE SUIVANTE:

DIRECTEUR
SERVICES D'INFORMATION SCIENTIFIQUES
QUARTIER GÉNÉRAL
DE LA DÉFENSE NATIONALE
OTTAWA, ONT. - CANADA K1A 0K2

Toute demande de document
doit être adressée à:

DIRECTEUR - SERVICES D'INFORMATION SCIENTIFIQUE
Ministère de la Défense nationale
Ottawa, Ontario
K1A 0K2

Téléphone: (613) 995-2971
Télécopieur: (613) 996-0392